Axonal and dendritic synaptotagmin isoforms revealed by a pHluorin-syt functional screen

Camin Dean[a,b,*], F. Mark Dunning[a], Huisheng Liu[a], Ewa Bomba-Warczak[a], Henrik Martens[c], Vinita Bharat[b], Saheeb Ahmed[b], and Edwin R. Chapman[a]
[a]Department of Neuroscience, Howard Hughes Medical Institute, University of Wisconsin, Madison, WI 53706;
[b]European Neuroscience Institute, 37077 Göttingen, Germany; [c]Synaptic Systems GmbH, 37079 Göttingen, Germany

ABSTRACT **The synaptotagmins (syts) are a family of molecules that regulate membrane fusion. There are 17 mammalian syt isoforms, most of which are expressed in the brain. However, little is known regarding the subcellular location and function of the majority of these syts in neurons, largely due to a lack of isoform-specific antibodies. Here we generated pHluorin-syt constructs harboring a luminal domain pH sensor, which reports localization, pH of organelles to which syts are targeted, and the kinetics and sites of exocytosis and endocytosis. Of interest, only syt-1 and 2 are targeted to synaptic vesicles, whereas other isoforms selectively recycle in dendrites (syt-3 and 11), axons (syt-5, 7, 10, and 17), or both axons and dendrites (syt-4, 6, 9, and 12), where they undergo exocytosis and endocytosis with distinctive kinetics. Hence most syt isoforms localize to distinct secretory organelles in both axons and dendrites and may regulate neuropeptide/neurotrophin release to modulate neuronal function.**

Monitoring Editor
Patrick Brennwald
University of North Carolina

Received: Aug 18, 2011
Revised: Feb 17, 2012
Accepted: Feb 29, 2012

INTRODUCTION

Members of the synaptotagmin (syt) protein family are likely to regulate a variety of membrane-trafficking events in cells. Syts contain a luminal tail, a transmembrane domain, and two cytoplasmic C2 domains (Perin *et al.*, 1991; Sutton *et al.*, 1995). Calcium-sensing by the C2 domains induces binding of some isoforms to lipids and soluble *N*-ethylmaleimide–sensitive factor attachment protein receptor proteins (Brose *et al.*, 1992; Chapman *et al.*, 1995; Schiavo *et al.*, 1997; Bhalla *et al.*, 2008), which promotes fusion and exocytosis of vesicle cargo (Chapman, 2008). The best-characterized isoform is syt-1, which is present on synaptic vesicles and is essential for fast synaptic transmission (DiAntonio and Schwarz, 1994; Geppert *et al.*, 1994; Littleton *et al.*, 1994). However, less is known concerning additional mammalian syt isoforms in neurons. All 17 isoforms have been detected in brain at the level of mRNA, except for syt-8, 14, and 15 (Lein *et al.*, 2007; Mittelsteadt *et al.*, 2009). Of importance, syt mRNAs are expressed in hippocampal neurons, except for syt-2, which is functionally redundant with syt-1 (Stevens and Sullivan, 2003), and expressed in distinct brain areas (Ullrich *et al.*, 1994; Marqueze *et al.*, 1995). Thus hippocampal neurons provide a valid model system for study of the localization and function of these syt isoforms.

Whereas syt-1 is present on synaptic vesicles, syt-4 was recently localized to neurotrophin-containing dense-core vesicles in hippocampal neurons, where it negatively regulates BDNF (brain-derived neurotrophic factor) release (Dean *et al.*, 2009). Synaptic vesicles (harboring syt-1) and dense-core vesicles (harboring syt-4) have distinct recycling characteristics in hippocampal neurons, as revealed by pHluorin reporters. pHluorins fused to a luminal domain of synaptic vesicles exhibit a fast depolarization–induced increase in fluorescence, corresponding to exocytosis, followed by a slower decay to baseline fluorescence within 60–90 s, indicating endocytosis and reacidification of vesicles (Sankaranarayanan and Ryan, 2000; Granseth *et al.*, 2006). In contrast, pHluorin–syt-4 exhibits fluorescence changes in response to depolarization in both axons and dendrites, and axonal events have slower rise and decay kinetics than do synaptic vesicle pHluorins. In addition, pHluorin–syt-4 fluorescence often remains elevated for several minutes following stimulation (Dean *et al.*, 2009).

This article was published online ahead of print in MBoC in Press (http://www.molbiolcell.org/cgi/doi/10.1091/mbc.E11-08-0707) on March 7, 2012.

*Present address: European Neuroscience Institute, 37077 Göttingen, Germany.
Address correspondence to: Edwin R. Chapman (chapman@wisc.edu).

Abbreviations used: BDNF, brain-derived neurotrophic factor; BSA, bovine serum albumin; DIV, days in vitro; EPSC, excitatory postsynaptic current; GFP, green fluorescent protein; HEPES, 4-(2-hydroxyethyl)-1-piperazineethanesulfonic acid; ROI, region of interest.

These unique recycling characteristics enable a distinction of syts localized to these and other organelles. Here we performed a pHluorin "screen" of syt isoforms in hippocampal neurons to determine 1) whether they recycle in response to depolarization, 2) whether they undergo exo/endocytosis in axons, dendrites, or both, and 3) whether their recycling characteristics suggest localization to synaptic vesicles or to other vesicle subtypes. Syts-1–7, 9–12, and 17 were tested. Of interest, we found that five syts (syt-1, 2, 5, 7, and 17) underwent exocytosis exclusively in axons, but only syt-1 and 2 exhibited recycling characteristics indicative of localization to synaptic vesicles, whereas syt-5, 7, and 17 displayed unique recycling kinetics suggesting localization to distinct vesicle subtypes. Two syts (syt-3 and 11) recycled exclusively in dendrites, and four (syt-4, 6, 9, and 12) recycled in both axons and dendrites. Our results suggest that the syts have diverged to regulate activity-dependent fusion of a wide variety of distinct vesicle subtypes and may therefore modulate synaptic transmission indirectly via regulation of release of neuropeptides or neurotrophins.

RESULTS

To assess the membrane-recycling properties of the syts, we fused a pH-sensitive green fluorescent protein (GFP) variant, pHluorin, to the luminal domain of each isoform with a preprolactin leader sequence and a linker to promote efficient targeting (Fernandez-Alfonso *et al.*, 2006). Inside the lumen of acidic vesicles, pHluorin fluorescence is quenched. When these vesicles undergo exocytosis, their luminal domains are exposed to the more basic extracellular solution, and they become fluorescent. Subsequent endocytosis results in vesicle reacidification and a corresponding decay in fluorescence. Thus recycling events can be detected as sites of transient increases in fluorescence.

To determine whether recycling occurred in axons or dendrites of hippocampal neurons, we examined transfected cells in which these processes could clearly be identified using prior low-magnification imaging, in which axons extend longer processes than do dendrites (Supplemental Figure S1). In cases in which the two types of processes were difficult to distinguish morphologically, retrospective immunostaining for GFP to mark pHluorin-syt and MAP-2 to mark dendrites was used. Of interest, in these immunostaining experiments, most syts were detected in both axonal and dendritic compartments (Supplemental Figure S2); only pHluorin-syt time-lapse imaging experiments during depolarization revealed recycling of specific syts in distinct compartments.

We first compared the recycling characteristics of synaptophysin (syp)-pHluorin, which is exclusively localized to synaptic vesicles (Granseth *et al.*, 2006), and of pHluorin–syt-4, which is present on neurotrophin-containing dense-core vesicles (Dean *et al.*, 2009). Both of these fusion proteins have been validated to localize identically to their endogenous counterparts (Granseth *et al.*, 2006; Dean *et al.*, 2009). Hippocampal neurons were transfected with these fusion constructs, and transfected cells, which could be detected by faint fluorescence prior to stimulation, were imaged during depolarization with 45 mM KCl, which has been shown to efficiently induce exocytosis of both synaptic vesicles and neurotrophin-containing dense-core vesicles (Hartmann *et al.*, 2001; Kolarow *et al.*, 2007; Dean *et al.*, 2009).

Depolarization caused a rapid fluorescence increase at presynaptic boutons in axons of syp-pHluorin–transfected neurons, with no significant fluorescence or change in fluorescence detected in dendrites (Figure 1A). This increase in fluorescence in axons decayed (corresponding to endocytosis and reacidification) within 90 s, as previously shown for this reporter of synaptic vesicle recycling (Granseth *et al.*, 2006). pHluorin–syt-4 fluorescence also increased in axons in response to depolarization and then decreased, but with slower kinetics than for syp-pHluorin (Figure 1B). In addition, unlike syp-pHluorin responses, pHluorin–syt-4 axonal events were not always coincident with the onset of depolarization. Moreover, pHluorin-syt-4 vesicles also underwent exocytosis in dendrites (Figure 1C), where they exhibited either a small, fast rise and decay (Figure 1D) or a large, fast increase in fluorescence, which remained elevated in the presence of depolarizing solution (Dean *et al.*, 2009; Figure 1E). These data confirm that synaptic vesicle– and dense-core vesicle–localized proteins have spatially and temporally distinct pHluorin responses.

Of all the syt isoforms tested, only two—syt-1 and syt-2—exhibited pHluorin responses indicative of localization to synaptic vesicles. pHluorin–syt-1 increased in fluorescence immediately following depolarization and then decayed back to baseline with kinetics nearly identical to that of syp-pHluorin (Figure 2A). pHluorin–syt-2 also exhibited recycling characteristics indicating localization to synaptic vesicles (Figure 2B), as expected, since syt-2 has been shown to be functionally redundant with syt-1 (Stevens and Sullivan, 2003), but is localized to distinct brain areas where syt-1 is absent (Ullrich *et al.*, 1994; Marqueze *et al.*, 1995).

We found that three other syts—syt-5, 7, and 17—were also exclusively recycled in axons (Figure 3). However, the pHluorin characteristics of these syts were not synaptic vesicle like. Syt-10 was the only syt (in addition to syt-8; unpublished data) that did not exhibit a fluorescence change in response to depolarization (Figure 3A) in either the absence or presence of bafilomycin to block the vacuolar ATPase (Figure 3A, inset). The majority of pHluorin–syt-10 was localized to the plasma membrane in nondepolarizing conditions in hippocampal neurons. Syt-10 is most highly expressed in the olfactory bulb, where it was reported to regulate insulin-like growth factor 1 secretion (Cao *et al.*, 2011). In the hippocampus syt-10 is specifically up-regulated in a subset of neurons following seizure activity (Babity *et al.*, 1997). Thus pHluorin–syt-10 may be "inactive" in normal conditions in the majority of hippocampal neurons and specifically invoked to recycle in subsets of neurons under conditions of high activity.

pHluorin–syt-5 was also visible on the plasma membrane, prior to depolarization, exclusively in axons (Figure 3B), and this isoform exhibited increases in fluorescence at select sites, coincident with depolarization. These fluorescence responses were large in comparison with the majority of syt isoforms, with a slow rise time (Supplemental Figure S3, A and B) reminiscent of the dense-core vesicle recycling characteristics previously observed for pHluorin–syt-4 in axons. pHluorin–syt-7 also exhibited fluorescence increases exclusively in axons (Figure 3C), which were of smaller magnitude than for any other axonal syt isoform (Supplemental Figure S3A) and remained elevated following depolarization for at least several minutes. These observations suggest that syt-7 is present on internal vesicles that undergo exocytosis, as reported in nonneuronal cells (Wang *et al.*, 2005), and that it is not exclusively localized to the plasma membrane as proposed previously (Sugita *et al.*, 2001). Syt-7 was also previously localized to lysosomes in nonneuronal cells (Reddy *et al.*, 2001; Roy *et al.*, 2004). Thus it is possible that the pHluorin–syt-7 response following depolarization corresponds to lysosomal fusion (Arantes and Andrews, 2006).

pHluorin–syt-17 was also localized predominantly to axons, but this isoform had characteristics distinct from those of all other axonally localized isoforms. Diffusely distributed plasma membrane fluorescence was not observed, but rapidly trafficking vesicles were clearly visible in nondepolarizing conditions (Figure 3D and Supplemental Movie S1). Syt-17 is predicted to be membrane associated but to lack a transmembrane domain (Craxton, 2010). Thus the

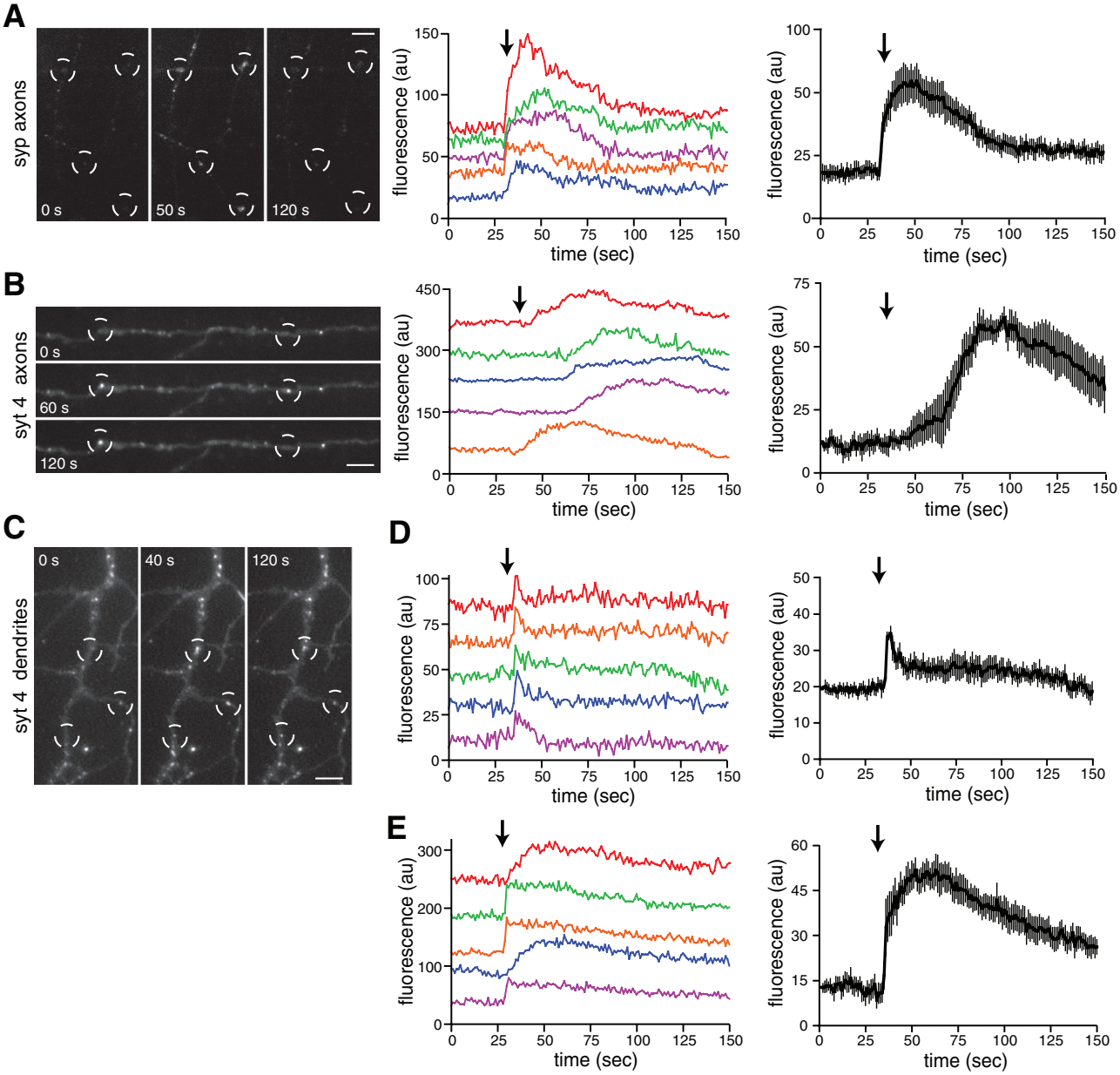

FIGURE 1: Synaptic vesicle–pHluorins and dense-core vesicle–pHluorins have distinct fluorescence characteristics. (A) Axonal regions of a synaptophysin-pHluorin–transfected neuron before and after depolarization (left). Sample regions that change fluorescence during depolarization are indicated with hatched white circles. Middle and right, sample and average fluorescence, respectively, during depolarization. Arrow indicates addition of 45 mM KCl to depolarize neurons. (B) Axon of a pHluorin-syt-4–transfected neuron before, during, and after depolarization, with sites of fluorescence change indicated (left). Sample (middle) and average (right) fluorescence traces of puncta before, during, and after depolarization. (C) Dendrites of a pHluorin-syt-4 transfected–neuron before, during, and after depolarization. (D) Sample (left) and average (right) traces of small, fast dendritic events. (E) Sample (left) and average (right) traces of large, slow dendritic events (n = 27–57 ROIs from three cultures; error bars indicate SEM). Scale bars, 5 μm.

pHluorin fused to syt-17 may be cytoplasmic, resulting in strong fluorescence. Alternatively, these vesicles may have a higher pH than synaptic vesicles and could correspond to nonacidified dense-core vesicles or signaling endosomes (Cosker *et al.*, 2008). pHluorin–syt-17 fluorescence did increase at isolated puncta in response to depolarization, suggesting that syt-17 is an integral vesicle protein, but at far fewer sites than other syt isoforms. These pHluorin responses were characterized by fast, large increases in fluorescence (Supplemental Figure S3), which remained elevated in the presence of depolarizing solution (Figure 3D).

Two syt isoforms exhibited pHluorin responses upon depolarization exclusively in dendrites: syt-3 and syt-11. Syt-3 was the only isoform to undergo endocytosis, instead of exocytosis, in response to depolarization. In resting conditions syt-3 was present in a punctate pattern resembling postsynaptic sites in both proximal (Figure 4A) and distal (Figure 4B) dendrites. Following depolarization, the fluorescence of these puncta decayed exponentially (Figure 4C). This fluorescence decay corresponded to endocytosis, since perfusion with NH_4Cl to neutralize all internal acidic compartments resulted in recovery of fluorescence at these sites (Supplemental

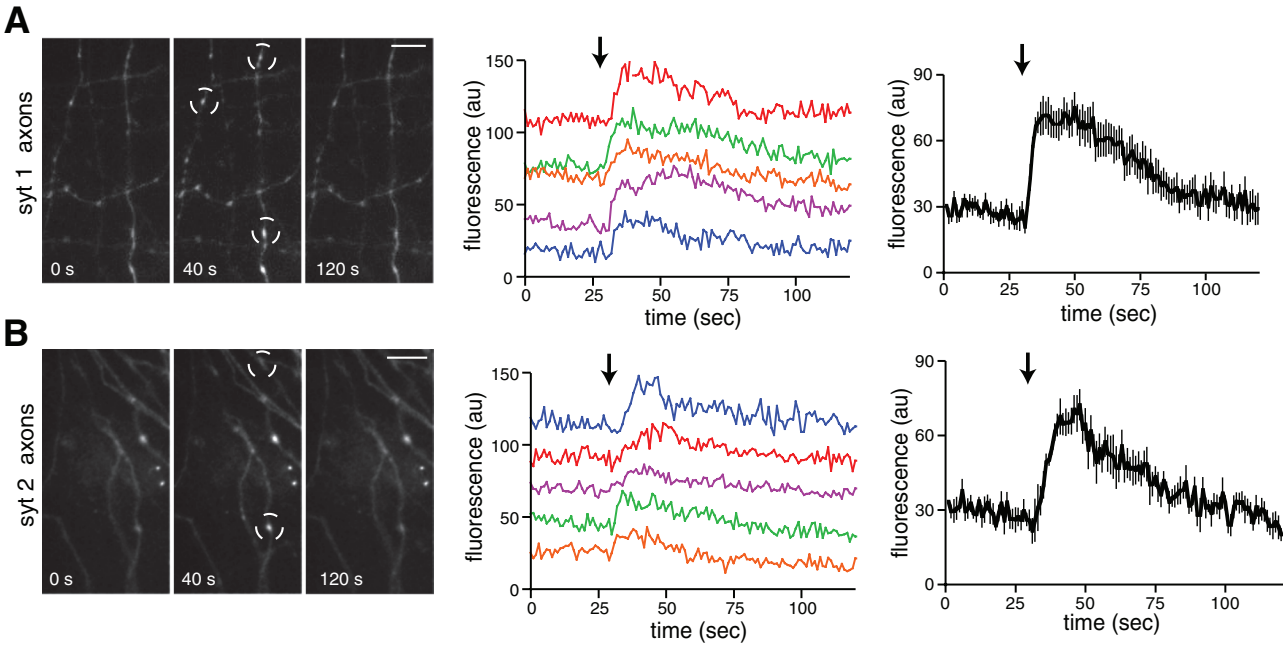

FIGURE 2: Syt-1 and syt-2 are the only isoforms that exhibit synaptic vesicle–like pHluorin responses. (A) Axonal regions of a pHluorin-syt-1–transfected neuron (left), with sample (middle) and average (right) fluorescence traces during depolarization. (B) Axonal regions of a pHluorin-syt-2–transfected neuron (left), sample (middle), and average (right) fluorescence traces during depolarization (n = 27–30 ROIs from three cultures; error bars indicate SEM). Scale bars, 5 μm.

Figure S4), and the depolarization-induced fluorescence decay was abolished in the presence of bafilomycin to block reacidification (Figure 4C, inset). Syt-11–containing vesicles also recycled exclusively in dendrites but with very different kinetics compared with syt-3. Syt-11 vesicles were often visible prior to depolarization and exhibited small increases in fluorescence (Figure 4D and Supplemental Figure S3A), which decayed back to baseline within 60–90 s.

Three syt isoforms in addition to syt-4 exhibited pHluorin responses upon depolarization, in both axons and dendrites. Syt-6 was predominantly axonal (Figure 5A), with a relatively large proportion of pHluorin–syt-6 on the plasma membrane under resting conditions. Large increases in pHluorin–syt-6 fluorescence in axons were observed in response to depolarization (Supplemental Figure S3A), the majority of which remained elevated for at least 2–3 min following addition of high-potassium solution. Syt-6 was also present in a punctate pattern in dendrites (Figure 5B), and subsets of these puncta initially decreased and then increased in fluorescence following depolarization but with a magnitude approximately one-fourth the size of axonal events (Supplemental Figure S3A).

Although syt-9 mRNA is not present at high levels in hippocampus (Mittelsteadt *et al.*, 2009), our Western blot analysis of wild-type and syt-9–knockout mice indicates that syt-9 protein is present in this brain region (Supplemental Figure S5). Syt-9 exhibited several pHluorin characteristics that were similar to those of syt-4; vesicles were visible prior to stimulation, trafficked rapidly in both axons (Figure 6A) and dendrites (Figure 6B), and increased in fluorescence in both compartments in response to depolarization (Figure 6, A and B). We note that syt-9 was recently postulated to localize to synaptic vesicles, where it was reported to rescue fast synaptic transmission in syt-1 knockouts in cortical neurons (Xu *et al.*, 2007). However, we found that the same construct used in that study was poorly localized to synaptic sites in comparison to syt-1 (Figure 7, A and B) and failed to rescue fast synaptic transmission in hippocampal neurons from syt-1–knockout mice (Figure 7, C–H). This raises the possibility that this isoform may regulate dense-core vesicle release in the hippocampus.

Syt-12 also exhibited responses in both axons and dendrites. In axons pHluorin–syt-12 responded to depolarization with fluorescence increases, which remained elevated in depolarizing conditions (Figure 8A). In dendrites (Figure 8B), puncta were often visible prior to stimulation; they increased in fluorescence and then decayed back to baseline within 2 min, with kinetics exhibiting little variation between different puncta.

We also compared the plasma membrane versus intracellular (vesicular) distribution of each syt isoform. Bath application of pH 5.5 solution acts to quench pHluorin fluorescence on the extracellular surface of the plasma membrane, whereas addition of NH_4Cl acts to dequench internal pHluorins if they are localized in acidic compartments. These treatments can therefore be used to assess the relative amounts of surface versus internal pHluorin in neurons expressing different pHluorin-tagged syt isoforms. We selected sites that had undergone exo/endocytosis following depolarization and then successively perfused pH 5.5 and NH_4Cl solution and measured the fluorescence at these sites (Figure 9A); the percentage of surface versus internal pHluorin was plotted for each syt (Figure 9B, upper graph). Of interest, axonally recycling syts had higher amounts of surface expression compared with dendritic syts or to syts that recycled in both compartments. These findings indicate that, surprisingly, the recycling of syts in specific subcellular compartments can be predicted by the ratio of surface-to-internal protein levels. As mentioned, both syt-7 and syt-3 exhibited a significant amount of internal fluorescence and thus are likely not exclusively plasma membrane localized, as previously suggested (Sudhof, 2002). We note that the surface fraction of syt-1 ranges between ~25 and 33% following field stimulation (Fernandez-Alfonso *et al.*, 2006; Wienisch and Klingauf, 2006). The slightly higher surface fraction detected in the present study (43.7 ± 15.3%) may be a result of prior

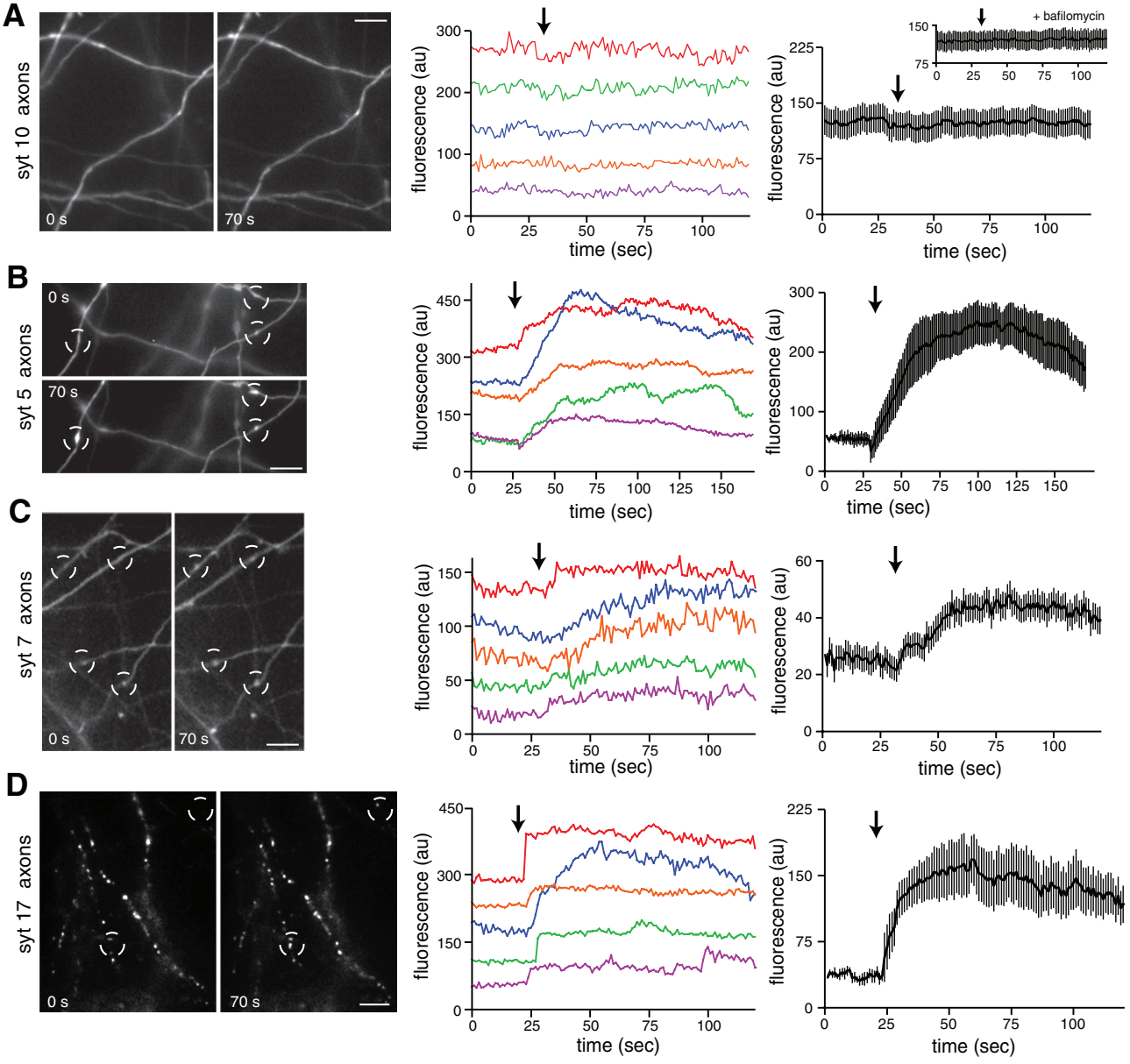

FIGURE 3: Syt-5, 7, and 17 undergo exocytosis exclusively in axons, with distinct kinetics. (A) pHluorin-syt-10–transfected neurons before and after depolarization (left). Sample (middle) and average (right) fluorescence traces during depolarization. Inset shows average fluorescence traces during depolarization in the presence of bafilomycin to block reacidification of vesicles. (B) pHluorin–syt-5 in axons before and after depolarization, and sample and average fluorescence traces. (C) pHluorin–syt-7 in axons before and after depolarization, with sample and average fluorescence traces. (D) pHluorin–syt-17 vesicles in axons before and after depolarization, with sample and average traces of fluorescence at exocytotic sites (n = 30–60 ROIs from three cultures; error bars indicate SEM). Scale bars, 5 μm.

stimulation with high-potassium solution, which could promote a larger amount of surface expression of syt-1.

In addition, we assessed the amount of syt present in nonacidified internal compartments (fluorescence above background in the presence of pH 5.5 solution) for each isoform and found that syts with synaptic vesicle–like recycling kinetics exhibited higher fluorescence levels in nonacidic compartments than axonal syts localized to other vesicle subtypes (Figure 9B, lower graph). This analysis relies on comparison of fluorescence intensities between different syts, which might reflect differences in expression levels. To address this, we calculated the average total fluorescence (Figure 9C) in the presence of NH_4Cl, which should reflect the total expression level, for each isoform. Total fluorescence did not correlate with nonacidified internal fluorescence, suggesting that expression levels do not affect the relative amount of internal versus external syt. In addition, expression levels did not influence the recycling of syt isoforms in axons versus dendrites (Figure 9C).

As mentioned, in many cases syt isoform–specific antibodies are not yet available, and only antibodies against syt-1, 4, and 9 (in the current study) have been validated using knockouts. However, we tested the localization of a subset of isoforms using anti-syt-1, 3, 4, 5, 9, and 12 antibodies in hippocampal cultures colabeled with MAP2 to mark dendrites (Figure 10A) or with synaptophysin to mark synaptic sites (Figure 10B). We found that syt-1 and syt-3

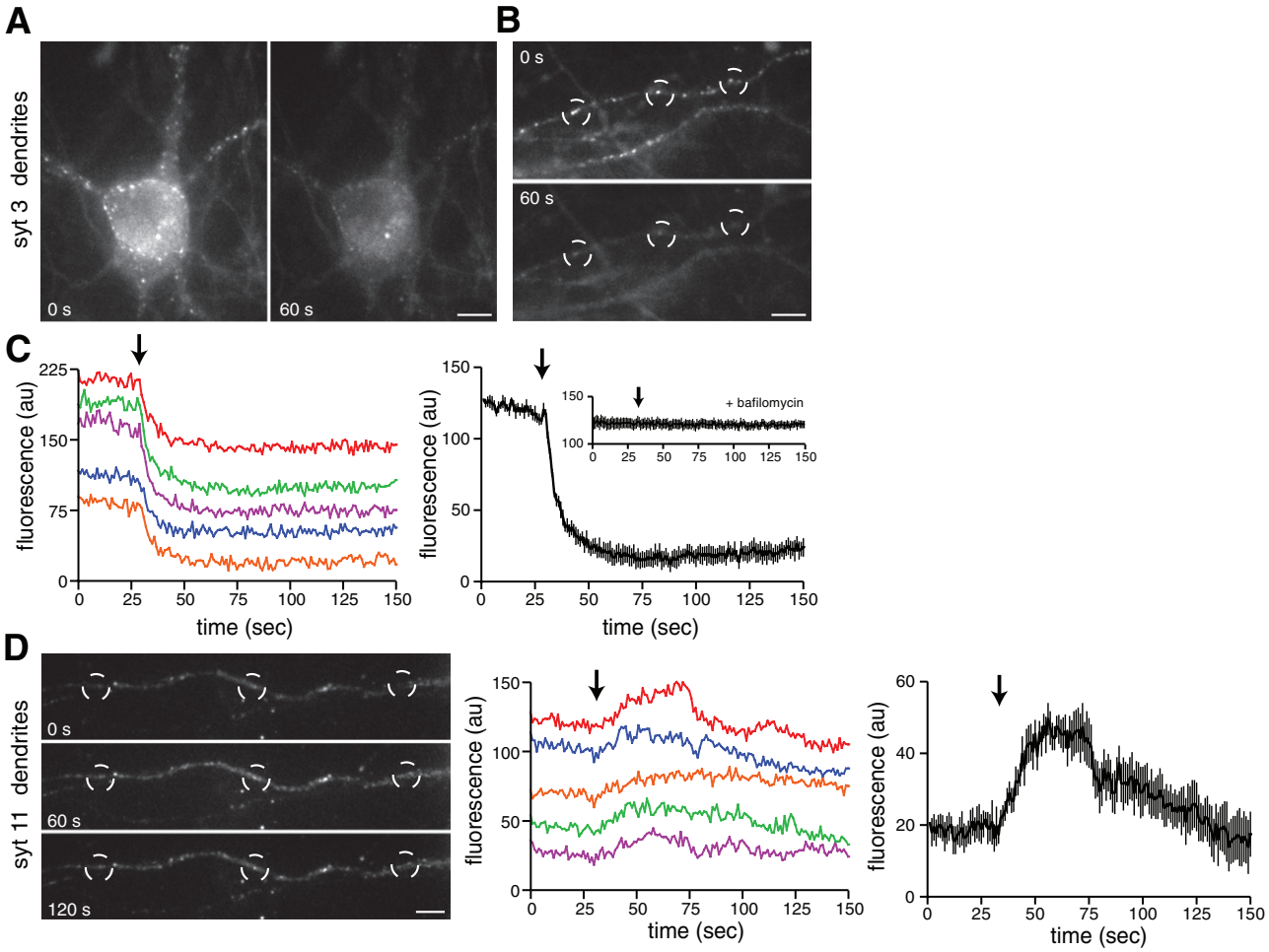

FIGURE 4: Syt-3 and 11 recycle in dendrites, where they exhibit unique pHluorin responses upon depolarization. (A) Cell body and proximal dendrites of pHluorin-syt-3–transfected neuron before and after depolarization. (B) Distal dendrites of the same cell. Fluorescent puncta are visible prior to depolarization, which decrease in fluorescence upon depolarization. (C) Representative (left) and average (right) traces of puncta fluorescence decay during depolarization. Inset shows average fluorescence traces during depolarization in the presence of bafilomycin to block reacidification. (D) Dendrite of a pHluorin-syt-11–transfected neuron prior to, during, and following depolarization (left). Representative (middle) and average (right) fluorescence traces during depolarization (n = 30 ROIs from three cultures; error bars indicate SEM). Scale bars, 5 μm.

exhibited the greatest colocalization with synaptophysin at synapses, syt-9 and syt-12 showed an intermediate value, and syt-4 and syt-5 exhibited the least colocalization. In terms of localization to axons or dendrites, syt-3 and syt-4 exhibited the highest colocalization with MAP2 signal in dendrites, syt-5, syt-9, and syt-12 showed intermediate colocalization, and syt-1 overlapped the least with MAP2. These findings are largely in agreement with the pHluorin-syt results, in which syt-1 is present on synaptic vesicles marked with synaptophysin, syt-3 is predominantly localized to dendrites, and syt-4, 5, 9, and 12 are present at some but not all synaptic sites and have varying degrees of localization to dendrites in addition to axons.

In summary, using pHluorin-tagged syt isoform reporters, we assayed the site and kinetics of recycling in response to depolarization of vesicles harboring each isoform to determine whether they recycle in axons and/or dendrites and to discern whether they are targeted to synaptic vesicles. We found that subsets of syts are differentially targeted to distinct vesicle subtypes in axons, dendrites, or both compartments (Table 1). Surprisingly, only two isoforms—syt-1 and syt-2—had pHluorin fluorescence responses characteristic of synaptic vesicles. The majority of syt isoforms appear to be localized to distinct secretory organelles in both axons and dendrites and thus have diverged to regulate exocytosis of a wide variety of vesicle subtypes in neurons.

DISCUSSION

The best-characterized synaptotagmin isoform is syt-1, which is present on synaptic vesicles and is essential for fast synaptic

Axons	Dendrites	Both	No response	Not in brain
syt-1 (SV)	syt-3	syt-4	syt-10	syt-8
syt-2 (SV)	syt-11	syt-6		syt-14
syt-5		syt-9		syt-15
syt-7		syt-12		
syt-17				

SV, synaptic vesicle.

TABLE 1: Summary of localization of syt isoforms based on pHluorin-syt characteristics.

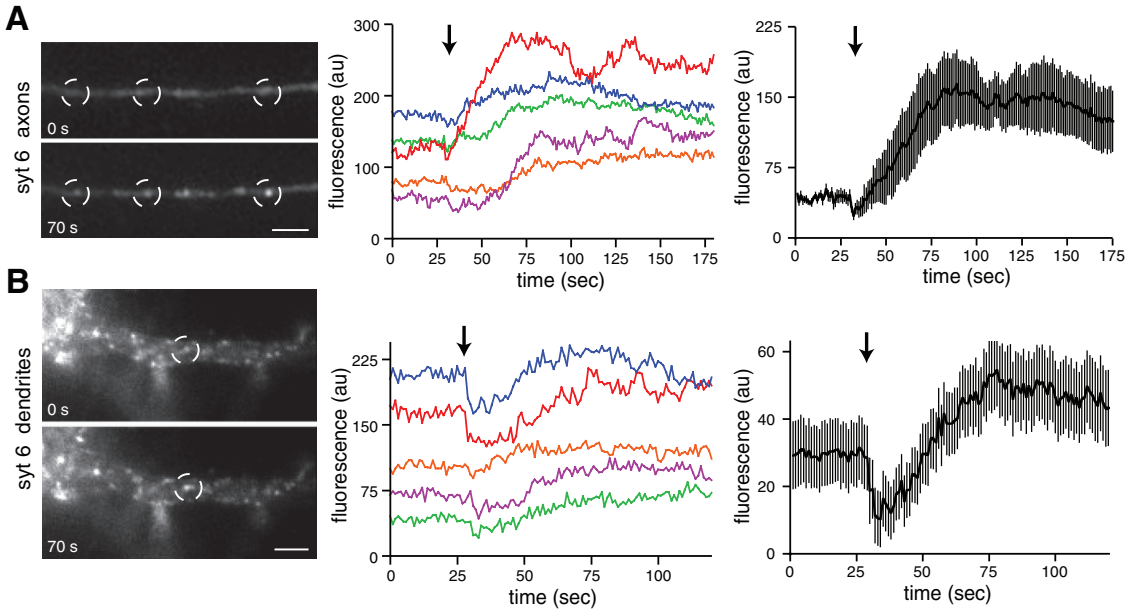

FIGURE 5: Syt-6 undergoes recycling in both axons and dendrites. (A) pHluorin–syt-6 in axons before and after depolarization (left). Representative (middle) and average (right) traces of fluorescence during depolarization. (B) pHluorin–syt-6 in dendrites (left), and sample and average fluorescence responses to depolarization (n = 27–30 ROIs from three cultures; error bars indicate SEM). Scale bars, 5 μm.

transmission (DiAntonio and Schwarz, 1994; Geppert *et al.*, 1994; Littleton *et al.*, 1994). The subsequent discoveries of additional isoforms led to speculation that different syts may regulate distinct aspects of synaptic vesicle function or be localized to distinct organelles to affect various intracellular trafficking events (Schiavo *et al.*, 1998; Marqueze *et al.*, 2000; Sudhof, 2002; Craxton, 2004). The syt isoforms have been well characterized in terms of their biochemical properties; different isoforms have distinct calcium sensitivities and kinetics of interactions with phospholipids (Bhalla *et al.*, 2005; Hui *et al.*, 2005). In addition, the distribution of syt isoform mRNAs has been well described (Mittelsteadt *et al.*, 2009). However, information regarding the subcellular localization and function of syt proteins has lagged behind, largely due to the inherent difficulties in generating isoform-specific antibodies.

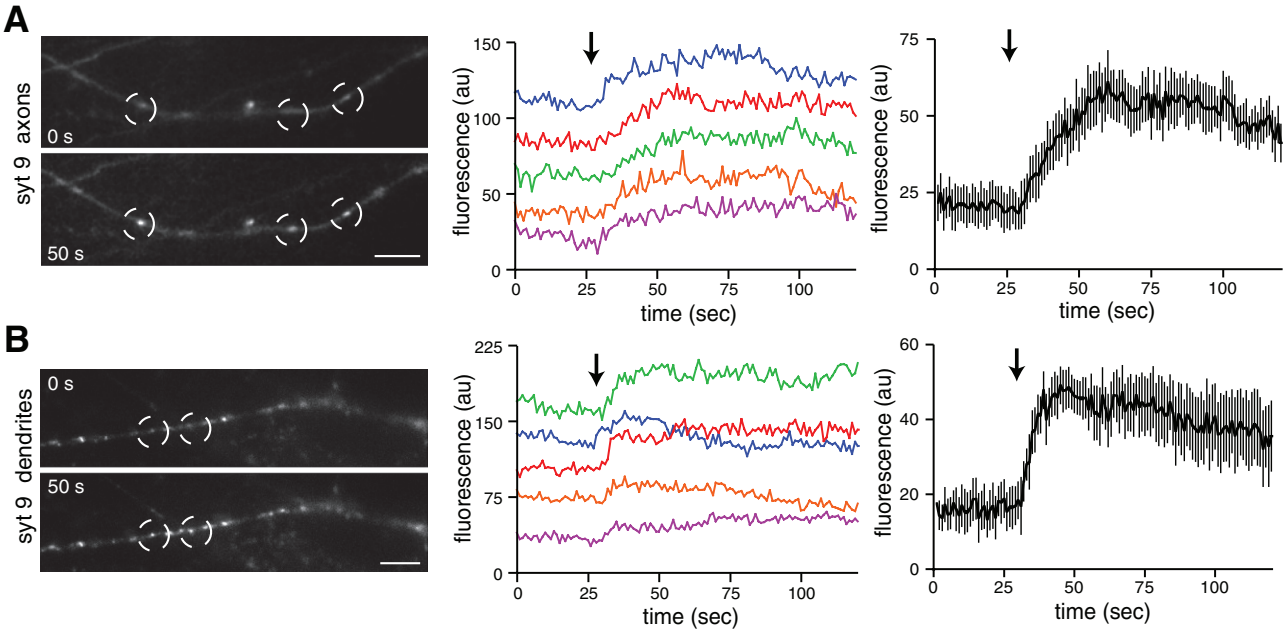

FIGURE 6: Syt-9–harboring vesicles recycle in both axons and dendrites. (A) pHluorin–syt-9 vesicles in axons before and after depolarization (left). Note that some puncta are visible prior to depolarization; these puncta traffic rapidly in anterograde and retrograde directions. (B) pHluorin–syt-9 in dendrites before and after depolarization (left), with sample and average fluorescence traces in response to depolarization (n = 30 ROIs from three cultures; error bars indicate SEM). Scale bars, 5 μm.

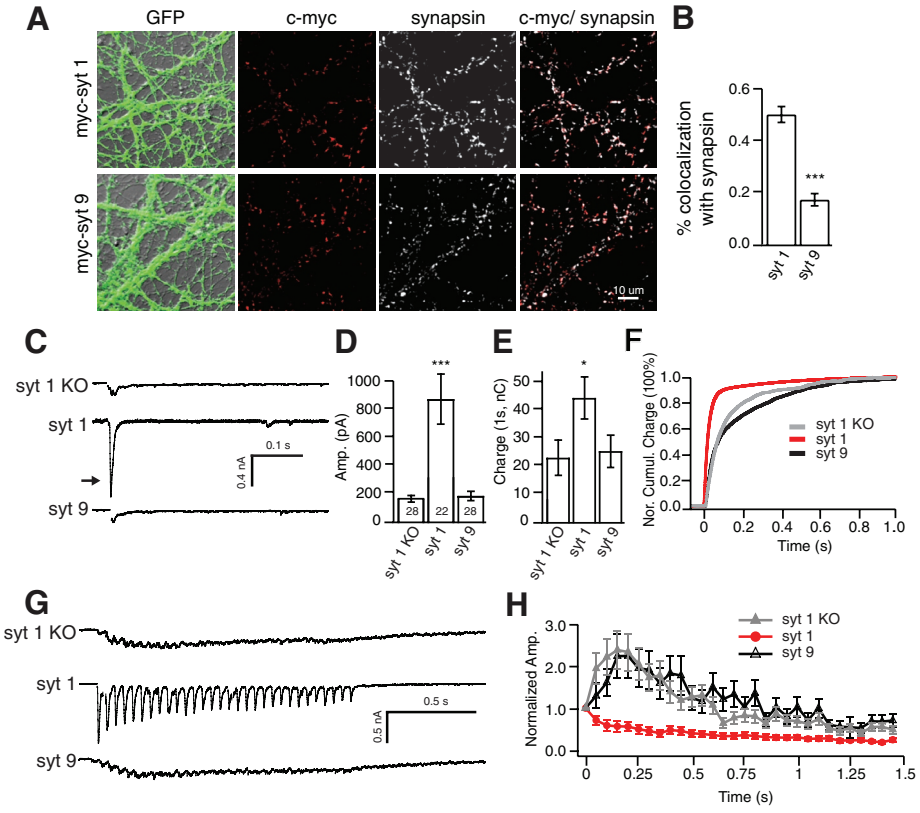

FIGURE 7: Syt-9 fails to rescue fast synaptic transmission in syt-1–knockout (KO) hippocampal neurons. (A) Hippocampal neurons infected with myc–syt-9 or myc–syt-1 lentiviral constructs were immunostained with anti-myc and anti-synapsin antibodies to mark synaptic vesicles. Scale bar, 10 μm. (B) Syt-1 colocalizes with the synaptic vesicle marker synapsin (0.48 ± 0.03; 850 puncta from four samples), whereas significantly less syt-9 colocalizes with synaptic vesicles (0.17 ± 0.02; 780 puncta from four samples), $p < 0.001$. (C) Evoked EPSCs from neurons in dissociated cultures were recorded as previously reported (Liu *et al.*, 2009). Syt-1 expression rescued fast synaptic transmission (arrow) in syt-1 KOs, but syt-9 failed to rescue. (D) Statistical analysis of EPSC amplitude (in pA; syt-1 KO, 150 ± 25; syt-1, 866 ± 179; syt-9, 170 ± 33) and charge (E) calculated over 1 s (in nC; syt-1KO, 22 ± 6; syt-1, 44 ± 9; syt-9, 25 ± 6). The number of neurons in each group (n) is indicated. (F) Normalized cumulative charge transfer further indicates that expression of syt-9 does not alter release kinetics in syt-1–knockout neurons. (G) Representative EPSC traces in response to high-frequency stimulation (30 action potentials at 20 Hz). No fast component of release was observed in syt-9–expressing syt-1–knockout neurons, whereas syt-1 fully rescued fast release in knockout neurons. (H) The peak amplitude of each EPSC was normalized to the first EPSC and plotted vs. time to assess short-term plasticity. There is no statistically significant difference between syt-9–rescue and syt-1–knockout neurons. All data shown represent mean ± SEM. *$p < 0.05$, ***$p < 0.001$.

A number of fusion events play important roles in either mediating or modulating synaptic transmission, including the exocytosis of synaptic vesicles (Heuser and Reese, 1973), recycling of adhesion molecules (Tai *et al.*, 2007), ion channels (Misonou and Trimmer, 2004) and postsynaptic receptors (Shi *et al.*, 1999; Linnarsson *et al.*, 2000; Park *et al.*, 2004), and release of neuropeptides (Baraban and Tallent, 2004) and neurotrophins (Figurov *et al.*, 1996). Specific synaptotagmins with distinct biochemical properties could differentially regulate these exocytotic and endocytotic events in response to calcium. Syt-3, for example, undergoes endocytosis exclusively in dendrites in response to depolarization, with kinetics similar to that of pHluorin-tagged postsynaptic receptors retrieved from the plasma membrane in response to *N*-methyl-D-aspartic acid treatment (Lin and Huganir, 2007; Gong and De Camilli, 2008). These pHluorin-tagged postsynaptic receptors initially endocytose and then exhibit a gradual recovery to the plasma membrane surface over the course of ~10 min. Syt-3 may therefore act to down-regulate surface expression of postsynaptic receptors to modulate synaptic strength.

Syt-6, which was also present in a punctate pattern in dendrites, initially decreased and then increased in fluorescence following depolarization. This could correspond to the initial internalization of a receptor in response to stimulation, followed by reinsertion into the plasma membrane.

In addition, a number of neurotrophins and neuropeptides are required for specific aspects of synaptic function (Baraban and Tallent, 2004; Figurov *et al.*, 1996). The depolarization-dependent exocytosis of BDNF, which is essential for the plasticity of neuronal circuits in the hippocampus (Korte *et al.*, 1995), has recently been found to occur through multiple modes (Dean *et al.*, 2009; Matsuda *et al.*, 2009) regulated by syt-4 (Dean *et al.*, 2009). Both the amount and duration of BDNF release affect synaptic function differentially (Rutherford *et al.*, 1998); precise regulation of the release kinetics of various neuropeptides and neurotrophins via distinct syt isoforms may therefore contribute to the plasticity of circuits.

Our findings from a "screen" of pHluorin-syt dynamics in neurons shed new light on the localization and function of the syt isoforms expressed in brain. This screen revealed differential localization of syts to distinct vesicle subtypes in axons versus dendrites, in which specific isoforms recycle only in axons, only in dendrites, or in both compartments. In addition, we found that the majority of syt isoforms are localized to vesicles with recycling characteristics different from those of synaptic vesicles. Five syts (syt-1, 2, 5, 7, and 17) undergo exocytosis exclusively in axons, but only syt-1 and 2 exhibited pHluorin responses indicating a localization to synaptic vesicles, whereas syt-5, 7, and 17 each displayed unique recycling kinetics, suggesting differential localization to distinct vesicle subtypes. Two syts (syt-3 and 11) recycled exclusively in dendrites, with distinct kinetics, and four syts (syt-4, 6, 9, and 12) were observed to undergo exo/endocytosis in both axons and dendrites. Different syt isoforms may have thus evolved to regulate fusion of distinct vesicle subtypes.

We found that pHluorin–syt-9 has characteristics similar to those of pHluorin–syt-4, where vesicles are visible prior to stimulation, traffic rapidly, and undergo recycling in both axons and dendrites. However, pHluorin–syt-9 vesicles fuse coincident with depolarization in axons, whereas there was often a delay prior to fusion of syt-4 vesicles. In addition, pHluorin–syt-9 dendritic fluorescence responses remained elevated following stimulation, whereas fast pHluorin–syt-4 dendritic responses decayed to baseline within 20 s. These observations are consistent with the ability of syt-9 to promote fusion (Bhalla *et al.*, 2008), possibly of neurotrophin- or neuropeptide-containing vesicles, whereas syt-4 inhibits their fusion (Dean *et al.*, 2009).

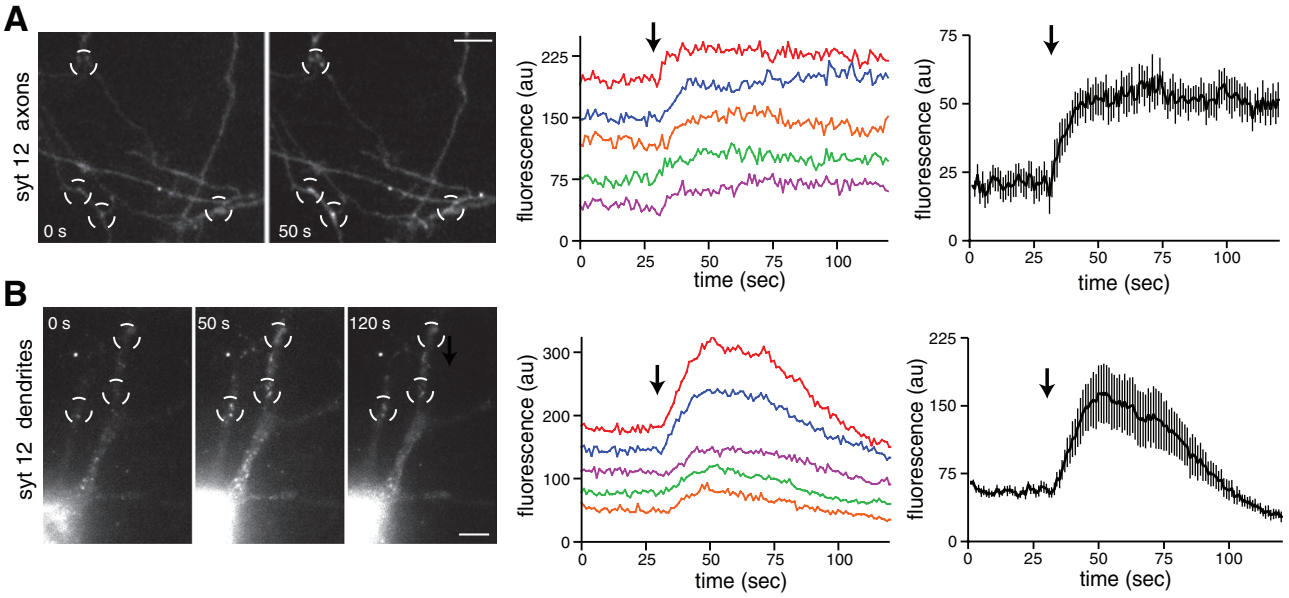

FIGURE 8: pHluorin-syt–12 harboring vesicles recycle in both axons and dendrites. (A) Axons of a pHluorin-syt-12–transfected neuron before and after depolarization (left), and sample and average fluorescence traces of pHluorin-syt-12 responses. (B) Dendritic regions of pHluorin-syt-12–transfected neurons before and 50 and 120 s after depolarization (left). Representative (middle) and average (right) fluorescence traces in response to depolarization (n = 30 ROIs from three cultures; error bars indicate SEM). Scale bars, 5 μm.

Syt-4 is one of four syt isoforms, in addition to syt-8, 11, and 12, that do not appear to sense Ca^{2+} and thus may act to inhibit fusion in neurons (Bhalla *et al.*, 2008), thereby conferring exocytosis with additional regulation. The pHluorin-syt-9 results in combination with the inability of syt-9 to substitute for syt-1 on synaptic vesicles to rescue fast transmission in syt-1 knockouts (Figure 7) raises the possibility that this isoform may regulate dense-core vesicle release. We note that syt-9 was recently postulated to localize to synaptic vesicles, in which it was reported to rescue fast synaptic transmission in syt-1 knockouts (Xu *et al.*, 2007). However, we found that the same construct used in that study was poorly localized to synaptic sites in comparison to syt-1 (Figure 7, A and B) and failed to rescue fast synaptic transmission in syt-1 knockouts (Figure 7, C–H). A possible explanation for this discrepancy is that syt-9 may be localized to distinct vesicle subtypes in hippocampus compared with the striatum, since Xu *et al.* focused on inhibitory postsynaptic currents recorded from striatal neurons and our study tested the effects of syt-9 on excitatory postsynaptic currents (EPSCs) from hippocampal neurons. Given the finding that syt-9 is present in hippocampus and syt-1 knockouts lack fast synchronous synaptic transmission in hippocampus (Geppert *et al.*, 1994; Liu *et al.*, 2009), we can exclude syt-9 as a fast synchronous calcium sensor for synaptic transmission in hippocampus.

The observation that pHluorin–syt-12 vesicle recycling occurs in both axons and dendrites with kinetics distinct from those of synaptophysin-pHluorin and pHluorin-syt-1 also contrasts with a recent study in which syt-12 was localized to synaptic vesicles, where it increased spontaneous neurotransmitter release without affecting evoked release (Maximov *et al.*, 2007). It is possible, however, that syt-12 is localized, perhaps to a greater extent, to other vesicle subtypes. Mass spectrometry of purified synaptic vesicles identified syt-1, 2, 9, 12, and 17 on synaptic vesicles (Takamori *et al.*, 2006), but syt-9, 12, and 17 were detected at significantly lower levels than syt-1. Syt-1 comprises 6.9% of the total synaptic vesicle protein at 15 copies per vesicle, whereas the remaining syt-9, 12, and 17 combined made up only 2.3% of the total synaptic vesicle protein content and were estimated to be present at five copies per vesicle in total. These syts may be localized to other vesicle subtypes, perhaps in greater abundance, where they could indirectly affect synaptic transmission, as in the case of syt-4 (Dean *et al.*, 2009).

PHluorin-syt-7–harboring vesicles underwent exocytosis exclusively in axons but also with kinetics distinct from that of synaptic vesicles. Syt-7 was previously localized to lysosomes in nonneuronal cells, where it regulates calcium-triggered exocytosis and plasma membrane repair (Reddy *et al.*, 2001; Roy *et al.*, 2004), and to dense-core vesicles in PC12 cells (Wang *et al.*, 2005). However, a role of syt-7 in affecting neuronal function in brain has not been described; syt-7 knockouts were reported to exhibit unaltered neurotransmitter release and short-term plasticity (Maximov *et al.*, 2008).

For several syts (including syt-4, 9, 11, 12, and 17) highly mobile fluorescent (nonacidifed) vesicles were visible in nondepolarizing conditions and remained fluorescent in the presence of pH 5.5 solution (to quench surface fluorescence), suggesting localization to nonacidified internal compartments. These compartments could correspond to recycling or signaling endosomes, which can range in pH from 5.5 to 6.5 (Demaurex, 2002; Ibanez, 2007; Cosker *et al.*, 2008).

The fraction of each syt in the plasma membrane also differs, and, of interest, the localization of isoforms to axons versus dendrites can be predicted based on how much is in the plasma membrane. In addition, the fraction of each syt in acidic versus nonacidic internal organelles differs, further supporting the idea that different syts are localized to distinct organelles. Finally, we found that each syt isoform exhibits different kinetics of pHluorin fluorescence response to depolarization. Surprisingly, only two isoforms—syt-1 and 2—were localized to synaptic vesicles based on their pHluorin recycling kinetics, whereas many additional syt isoforms exhibited dense-core vesicle–like pHluorin responses. These syts may be localized to distinct neuropeptide or neurotrophin vesicles to regulate their release. We cannot exclude the possibility that the additional syt isoforms

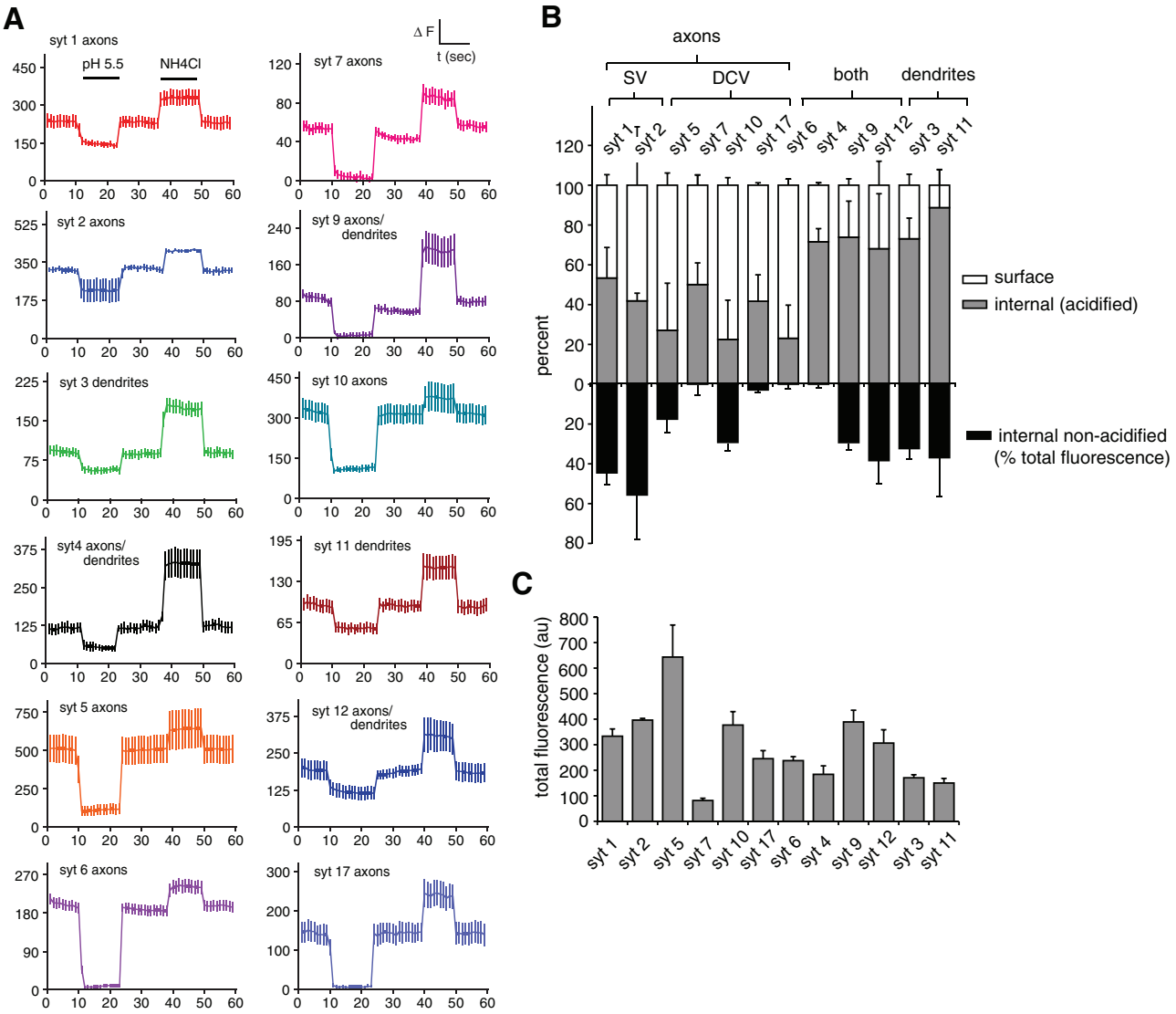

FIGURE 9: Surface vs. internal pHluorin-syt localization. (A) Fluorescence of the indicated pHluorin-syt isoforms during perfusion of pH 5.5 solution to quench surface fluorescence and NH_4Cl solution to alkalinize all internal acidic compartments and dequench internal pHluorin fluorescence. (B) Quantitation of percentage of surface vs. internal pHluorin-syt (top graph) and of nonacidified internal fluorescence compared between each isoform (expressed as percentage of total fluorescence). Isoforms are grouped in order of recycling exclusively in axons, in both axons and dendrites, or exclusively to dendrites. (C) Quantitation of total fluorescence for each syt isoform (total fluorescence above background in the presence of NH_4Cl).

may be localized to subsets of synaptic vesicles with pHluorin fluorescence kinetics distinct from that of vesicles containing synaptophysin, syt-1, and syt-2. However, this seems unlikely, given that synaptic vesicle populations lacking synaptophysin have not been reported and that individual synaptic vesicles in a mixed population all contain synaptophysin at similar copy numbers (Mutch *et al.*, 2011).

Analysis of chimeras composed of different domains of syt isoforms should make it possible to determine the structural elements that underlie differential targeting of this family of proteins to distinct organelles. Moreover, the finding that some isoforms are targeted to organelles that recycle in axons or in dendrites or are present in both classes of neurites opens the door to study aspects of polarized transport in neurons. Future studies will focus on how this polarity is achieved. In addition, a future challenge is to determine which cargoes are contained within these novel syt isoform–harboring vesicles and how the release of these cargoes might be regulated by the syts. The localization of specific syts to distinct axonal and dendritic vesicle subtypes suggests that they may regulate a broader range of exocytotic events than previously appreciated.

MATERIALS AND METHODS

Hippocampal neuron cultures

Rat hippocampi were isolated from E18-19 rats as described previously (Banker and Cowan, 1977). Hippocampi were treated with trypsin for 20 min at 37°C, triturated to dissociate cells, plated at 25,000–50,000 cells/cm^2 on polylysine-coated coverslips (Carolina Biological Supply, Burlington, NC), and cultured in Neurobasal supplemented with 2% B-27 and 2 mM Glutamax (Life Technologies, Invitrogen, Carlsbad, CA).

All procedures involving animals were performed in accordance with the guidelines of the National Institutes of Health, as approved

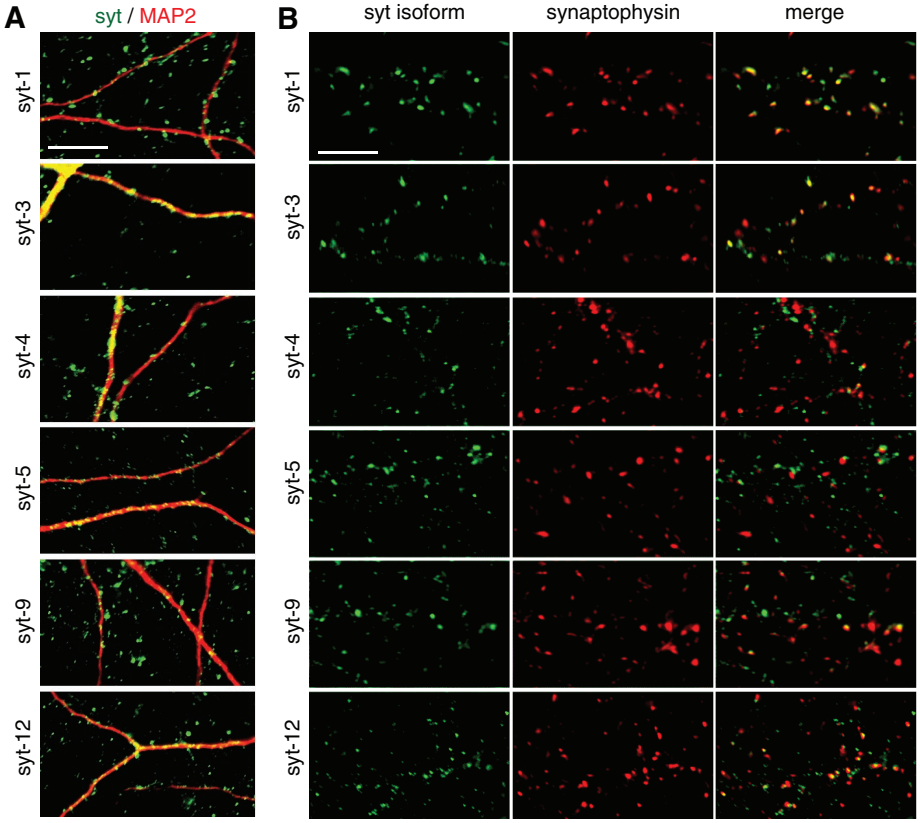

FIGURE 10: Localization of endogenous syts in hippocampal neurons. (A) Coimmunostaining of hippocampal neurons with anti-syt-1, 3, 4, 5, 9, and 12 (green) and anti-MAP2 (red) to mark dendrites. Percentage overlap of syt signal with MAP2 signal was as follows: 13 ± 2 (syt-1), 47 ± 16 (syt-3), 43 ± 2 (syt-4), 39 ± 8 (syt-5), 23 ± 4 (syt-9), and 24 ± 9 (syt-12). (B) Immunostains of anti-syt-1, 3, 4, 5, 9, and 12 with anti-synaptophysin to mark synaptic sites. Percentage overlap of syt signal with synaptophysin signal was as follows: 90 ± 4 (syt-1), 78 ± 1 (syt-3), 13 ± 3 (syt-4), 12 ± 1 (syt-5), 26 ± 5 (syt-9), and 54 ± 10 (syt-12). Scale bars, 10 µm.

by the Animal Care and Use Committee of the University of Wisconsin-Madison.

Antibodies and mammalian expression constructs

Antibodies used were as follows: polyclonal syt-1 (cat. #105102), syt-3 raised against amino acids 86–169 of human syt-3, syt-4 (cat. #105043), syt-5 raised against amino acids 74–147, syt-9 (cat. #105053), synaptophysin (Synaptic Systems, Göttingen, Germany), syt-12, GFP (Abcam, Cambridge, MA), MAP2 (Millipore, Billerica, MA; Synaptic Systems), and Alexa 405, Alexa 488, Alexa 546, and Alexa 647 secondaries (Invitrogen). pHluorin-syt-1 was provided by T. Ryan (Weill Medical College of Cornell University, New York, NY). Additional pHluorin-syt constructs were generated by replacing the syt-1 in pHluorin-syt-1 by PCR-amplified syts. Syt-2, 5–8, 10, and 11 were provided by M. Fukuda (Tohoku University, Sendai, Japan). Syt-3 was provided by S. Seino (Kobe University, Kobe, Japan). Syt-4 was provided by B. Hilbush (Roche Research Center, Nutley, NJ). Syt-9 was provided by M. Birnbaum (University of Pennsylvania, Philadelphia, PA). Syt-17 was provided by M. Craxton (MRC Laboratory, Cambridge, United Kingdom). A myc-tagged syt-9 lentiviral construct based on the pFUGW vector with the human polyubiquitin promoter was provided by T. Sudhof (Stanford University, Palo Alto, CA). Myc–syt-9 and myc–syt-1 were constructed by tagging syt-9 or syt-1 with a myc epitope and signal sequence at the N-terminus and subcloning into a double synapsin promoter lentiviral expression plasmid (provided by F. Gomez-Scholl, University of Seville, Seville, Spain). ImageJ software (National Institutes of Health, Bethesda, MD) was used to analyze the colocalization of myc-tagged syt-1 and syt-9 with anti-synapsin (Synaptic Systems).

Immunocytochemistry, image acquisition, quantitation, and statistical analysis

Cells were fixed with 4% paraformaldehyde, permeabilized with 0.1–0.2% Triton X-100 and 10% goat serum or 1% bovine serum albumin (BSA), blocked with 0.1% Triton X-100, 10% goat serum, or 10% BSA, and immunostained at room temp for 1–2 h or overnight at 4°C. Images were acquired on an Olympus FV1000 upright confocal microscope (Olympus, Center Valley, PA) with a 60×, 1.10 numerical aperture water immersion lens and a Zeiss Axiovert epifluorescence microscope with a 100× oil objective (Carl Zeiss, Jena, Germany). For quantitation of percentage colocalization, images were acquired with identical laser and gain settings and imported into MetaMorph (Molecular Devices, Sunnyvale, CA). Channels were thresholded separately to include all recognizable puncta. Percentage colocalization was determined as percentage of the total thresholded area of one channel (syt signal) that overlapped with the thresholded area of the corresponding channel (synaptophysin or MAP-2 signal).

Transfection of hippocampal neurons

Neurons growing on 12-mm coverslips in 24-well plates were transfected with Lipofectamine (Invitrogen) or calcium phosphate. For Lipofectamine transfection (at 5–6 d in vitro [DIV]), medium was removed, saved, and replaced with 500 µl of fresh medium. One microliter of Lipofectamine 2000 in 50 µl of Neurobasal medium and 0.5 µg of DNA in 50 µl of Neurobasal medium were incubated separately for 5 min and then mixed and incubated for 30 min at room temperature. This mixture was added to the well of neurons, incubated for 4 h at 37°C and 5% CO_2, and then removed and replaced with half saved medium and half fresh medium.

Neurons were transfected using calcium phosphate at 3–6 DIV as described previously (Dresbach *et al.*, 2003). Prior to transfection, medium was removed, saved, and replaced with 500 µl of 37°C Optimem (Life Technologies, Carlsbad, CA) and incubated for 30–60 min. A 105-µl amount of transfection buffer (274 mM NaCl, 10 mM KCl, 1.4 mM Na_2HPO_4, 15 mM glucose, 42 mM 4-(2-hydroxyethyl)-1-piperazineethanesulfonic acid [HEPES], pH 7.06) was added dropwise to a solution containing 7 µg of DNA and 250 mM $CaCl_2$, with gentle vortexing. This mixture was incubated for 20 min at room temperature, 30 µl was added per well, and the neurons were incubated for 60–90 min. This medium was then removed, cells were washed three times in 37°C Neurobasal medium, and saved medium was added back to the transfected cells.

pHluorin experiments

For time-lapse experiments, neurons were transferred to a live-imaging chamber (Warner Instruments, Hamden, CT) containing

bathing saline solution (140 mM NaCl, 5 mM KCl, 2 mM $CaCl_2$, 2 mM $MgCl_2$, 5.5 mM glucose, 20 mM HEPES, pH 7.3). Transfected cells (identified by faint GFP fluorescence in nondepolarizing conditions) in which axons and dendrites were clearly discernible by morphology were selected. Images were acquired at 1-s intervals and 500-ms exposure times, with 484/20-nm excitation and 517/20-nm emission filters, on a Nikon TE300 inverted microscope (Nikon, Melville, NY) with a Roper Scientific Photometrics Cascade IIB EM-CCD camera (Photometrics, Tucson, AZ) and Lambda DG-4 fast-switching light source interfaced with MetaMorph software. A baseline of 10 images was collected before addition of high-potassium buffer (100 mM NaCl, 45 mM KCl, 2 mM $CaCl_2$, 2 mM $MgCl_2$, 5.5 mM glucose, 20 mM HEPES, pH 7.3) to depolarize neurons. Axonal or dendritic regions were selected in MetaMorph, and the fluorescence intensity was plotted versus time. Puncta that did not exhibit any lateral movement during image acquisition and that exhibited a change in fluorescence in response to KCl were chosen for analysis; in the case of syt-10, which did not respond to depolarization, arbitrary regions of interest (ROIs) were chosen for comparison. Uniform, round, 1.5-μm-diameter ROIs were selected. For measurement of the surface versus internal amount of each syt isoform at exo/endocytotic sites, neurons were first depolarized to confirm that recycling events could be detected within the field of view. Subsequent sequential perfusion of pH 5.5, pH 7.3, and NH_4Cl solutions were then performed to determine surface and internal pHluorin at these same regions, using an MPS-2 multichannel perfusion system (World Precision Instruments, Sarasota, FL). For inhibition of the vesicular H^+ ATPase, neurons were incubated with 1 μM bafilomycin for 2 min (Calbiochem, La Jolla, CA) prior to imaging experiments.

Electrophysiology

Whole-cell patch-clamp recordings were made from dissociated syt-1–knockout hippocampal cultures (Geppert *et al.*, 1994). All recordings were done 12–15 d after neurons were plated on coverslips. The pipette solution consisted of 130 mM K-gluconate, 1 mM ethylene glycol tetraacetic acid, 5 mM Na-phosphocreatine, 2 mM Mg-ATP, 0.3 mM Na-GTP, 10 mM HEPES, and 5 mM QX-314, pH 7.3 (290 mOsm). Neurons were continuously perfused with extracellular solution consisting of 140 mM NaCl, 5 mM KCl, 1 mM $MgCl_2$, 10 mM glucose, 10 mM HEPES, pH 7.3 (300 mOsm), 50 μM D-2-amino-5-phosphonopentanoate, 0.1 mM picrotoxin, and 5 mM Ca^{2+}. All drugs were from Sigma-Aldrich (St. Louis, MO). The stimulating bipolar electrode was filled with extracellular solution. Neurons were voltage clamped at –70 mV with an EPC-10/2 amplifier (HEKA Electronics, Lambrecht/Pfalz, Germany). Only cells with series resistances of <15 MΩ, with 70–80% of this resistance compensated, were analyzed. Currents were acquired using PATCHMASTER software (HEKA), filtered at 2.9 kHz, and digitized at 10 kHz. Data were analyzed using Clampfit (Molecular Devices, Sunnyvale, CA), IGOR (WaveMetrics, Portland, OR), and ImageJ software. All experiments were carried out at room temperature.

Western blots

For Western blots of syt-9, brain regions were isolated from adult syt-9–knockout mice and wild-type littermates (Jackson Laboratory, Bar Harbor, ME; deposited by T. Sudhof) and homogenized in 320 mM sucrose and 4 mM HEPES, pH 7.4, using a Teflon glass homogenizer. Homogenates were centrifuged for 10 min at 1000 × *g* to pellet nuclei and insoluble debris. Supernatants were collected, and the protein concentration was determined according to a modified Lowry Peterson method that includes solubilization and precipitation of proteins by trichloroacetic acid (Peterson, 1977). Equal amounts of protein were loaded per lane for comparison of brain regions between wild-type and syt-9–knockout mice, resolved by SDS–PAGE, and analyzed by immunoblotting.

ACKNOWLEDGMENTS

We thank Sam Kwon for independent verification of pHluorin-syt results. This work was supported by National Institutes of Health Grant MH 61876 to E.R.C. and by Epilepsy Foundation, National Institutes of Health National Research Service Award, and Sofja Kovalevskaja Alexander von Humboldt and European Research Council grants to C.D. E.R.C is an investigator of the Howard Hughes Medical Institute.

REFERENCES

Arantes RM, Andrews NW (2006). A role for synaptotagmin VII-regulated exocytosis of lysosomes in neurite outgrowth from primary sympathetic neurons. J Neurosci 26, 4630–4637.

Babity JM, Armstrong JN, Plumier JC, Currie RW, Robertson HA (1997). A novel seizure-induced synaptotagmin gene identified by differential display. Proc Natl Acad Sci USA 94, 2638–2641.

Banker GA, Cowan WM (1977). Rat hippocampal neurons in dispersed cell culture. Brain Res 126, 397–342.

Baraban SC, Tallent MK (2004). Interneuron diversity series: interneuronal neuropeptides–endogenous regulators of neuronal excitability. Trends Neurosci 27, 135–142.

Bhalla A, Chicka MC, Chapman ER (2008). Analysis of the synaptotagmin family during reconstituted membrane fusion. Uncovering a class of inhibitory isoforms. J Biol Chem 283, 21799–21807.

Bhalla A, Tucker WC, Chapman ER (2005). Synaptotagmin isoforms couple distinct ranges of Ca2+, Ba2+, and Sr2+ concentration to SNARE-mediated membrane fusion. Mol Biol Cell 16, 4755–4764.

Brose N, Petrenko AG, Sudhof TC, Jahn R (1992). Synaptotagmin: a calcium sensor on the synaptic vesicle surface. Science 256, 1021–1025.

Cao P, Maximov A, Sudhof TC (2011). Activity-dependent IGF-1 exocytosis is controlled by the Ca(2+)-sensor synaptotagmin-10. Cell 145, 300–311.

Chapman ER (2008). How does synaptotagmin trigger neurotransmitter release. Annu Rev Biochem 77, 615–641.

Chapman ER, Hanson PI, An S, Jahn R (1995). Ca2+ regulates the interaction between synaptotagmin and syntaxin 1. J Biol Chem 270, 23667–23671.

Cosker KE, Courchesne SL, Segal RA (2008). Action in the axon: generation and transport of signaling endosomes. Curr Opin Neurobiol 18, 270–275.

Craxton M (2004). Synaptotagmin gene content of the sequenced genomes. BMC Genomics 5, 43.

Craxton M (2010). A manual collection of Syt, Esyt, Rph3a, Rph3al, Doc2, and Dblc2 genes from 46 metazoan genomes—an open access resource for neuroscience and evolutionary biology. BMC Genomics 11, 37.

Dean C, Liu H, Dunning FM, Chang PY, Jackson MB, Chapman ER (2009). Synaptotagmin-IV modulates synaptic function and long-term potentiation by regulating BDNF release. Nat Neurosci 12, 767–776.

Demaurex N (2002). pH Homeostasis of cellular organelles. News Physiol Sci 17, 1–5.

DiAntonio A, Schwarz TL (1994). The effect on synaptic physiology of synaptotagmin mutations in *Drosophila*. Neuron 12, 909–920.

Dresbach T, Hempelmann A, Spilker C, tom Dieck S, Altrock WD, Zuschratter W, Garner CC, Gundelfinger ED (2003). Functional regions of the presynaptic cytomatrix protein bassoon: significance for synaptic targeting and cytomatrix anchoring. Mol Cell Neurosci 23, 279–291.

Fernandez-Alfonso T, Kwan R, Ryan TA (2006). Synaptic vesicles interchange their membrane proteins with a large surface reservoir during recycling. Neuron 51, 179–186.

Figurov A, Pozzo-Miller LD, Olafsson P, Wang T, Lu B (1996). Regulation of synaptic responses to high-frequency stimulation and LTP by neurotrophins in the hippocampus. Nature 381, 706–709.

Geppert M, Goda Y, Hammer RE, Li C, Rosahl TW, Stevens CF, Sudhof TC (1994). Synaptotagmin I: a major Ca2+ sensor for transmitter release at a central synapse. Cell 79, 717–727.

Gong LW, De Camilli P (2008). Regulation of postsynaptic AMPA responses by synaptojanin 1. Proc Natl Acad Sci USA 105, 17561–17566.

Granseth B, Odermatt B, Royle SJ, Lagnado L (2006). Clathrin-mediated endocytosis is the dominant mechanism of vesicle retrieval at hippocampal synapses. Neuron 51, 773–786.
Hartmann M, Heumann R, Lessmann V (2001). Synaptic secretion of BDNF after high-frequency stimulation of glutamatergic synapses. EMBO J 20, 5887–5897.
Heuser JE, Reese TS (1973). Evidence for recycling of synaptic vesicle membrane during transmitter release at the frog neuromuscular junction. J Cell Biol 57, 315–344.
Hui E, Bai J, Wang P, Sugimori M, Llinas RR, Chapman ER (2005). Three distinct kinetic groupings of the synaptotagmin family: candidate sensors for rapid and delayed exocytosis. Proc Natl Acad Sci USA 102, 5210–5214.
Ibanez CF (2007). Message in a bottle: long-range retrograde signaling in the nervous system. Trends Cell Biol 17, 519–528.
Kolarow R, Brigadski T, Lessmann V (2007). Postsynaptic secretion of BDNF and NT-3 from hippocampal neurons depends on calcium calmodulin kinase II signaling and proceeds via delayed fusion pore opening. J Neurosci 27, 10350–10364.
Korte M, Carroll P, Wolf E, Brem G, Thoenen H, Bonhoeffer T (1995). Hippocampal long-term potentiation is impaired in mice lacking brain-derived neurotrophic factor. Proc Natl Acad Sci USA 92, 8856–8860.
Lein ES *et al*. (2007). Genome-wide atlas of gene expression in the adult mouse brain. Nature 445, 168–176.
Lin DT, Huganir RL (2007). PICK1 and phosphorylation of the glutamate receptor 2 (GluR2) AMPA receptor subunit regulates GluR2 recycling after NMDA receptor-induced internalization. J Neurosci 27, 13903–13908.
Linnarsson S, Willson CA, Ernfors P (2000). Cell death in regenerating populations of neurons in BDNF mutant mice. Brain Res Mol Brain Res 75, 61–69.
Littleton JT, Stern M, Perin M, Bellen HJ (1994). Calcium dependence of neurotransmitter release and rate of spontaneous vesicle fusions are altered in *Drosophila* synaptotagmin mutants. Proc Natl Acad Sci USA 91, 10888–10892.
Liu H, Dean C, Arthur CP, Dong M, Chapman ER (2009). Autapses and networks of hippocampal neurons exhibit distinct synaptic transmission phenotypes in the absence of synaptotagmin I. J Neurosci 29, 7395–7403.
Marqueze B, Berton F, Seagar M (2000). Synaptotagmins in membrane traffic: which vesicles do the tagmins tag? Biochimie 82, 409–420.
Marqueze B, Boudier JA, Mizuta M, Inagaki N, Seino S, Seagar M (1995). Cellular localization of synaptotagmin I, II, and III mRNAs in the central nervous system and pituitary and adrenal glands of the rat. J Neurosci 15, 4906–4917.
Matsuda N, Lu H, Fukata Y, Noritake J, Gao H, Mukherjee S, Nemoto T, Fukata M, Poo MM (2009). Differential activity-dependent secretion of brain-derived neurotrophic factor from axon and dendrite. J Neurosci 29, 14185–14198.
Maximov A, Lao Y, Li H, Chen X, Rizo J, Sorensen JB, Sudhof TC (2008). Genetic analysis of synaptotagmin-7 function in synaptic vesicle exocytosis. Proc Natl Acad Sci USA 105, 3986–3991.
Maximov A, Shin OH, Liu X, Sudhof TC (2007). Synaptotagmin-12, a synaptic vesicle phosphoprotein that modulates spontaneous neurotransmitter release. J Cell Biol 176, 113–124.
Misonou H, Trimmer JS (2004). Determinants of voltage-gated potassium channel surface expression and localization in mammalian neurons. Crit Rev Biochem Mol Biol 39, 125–145.
Mittelsteadt T, Seifert G, Alvarez-Baron E, Steinhauser C, Becker AJ, Schoch S (2009). Differential mRNA expression patterns of the synaptotagmin gene family in the rodent brain. J Comp Neurol 512, 514–528.
Mutch SA *et al*. (2011). Protein quantification at the single vesicle level reveals that a subset of synaptic vesicle proteins are trafficked with high precision. J Neurosci 31, 1461–1470.
Park M, Penick EC, Edwards JG, Kauer JA, Ehlers MD (2004). Recycling endosomes supply AMPA receptors for LTP. Science 305, 1972–1975.
Perin MS, Johnston PA, Ozcelik T, Jahn R, Francke U, Sudhof TC (1991). Structural and functional conservation of synaptotagmin (p65) in *Drosophila* and humans. J Biol Chem 266, 615–622.
Peterson GL (1977). A simplification of the protein assay method of Lowry et al. which is more generally applicable. Anal Biochem 83, 346–356.
Reddy A, Caler EV, Andrews NW (2001). Plasma membrane repair is mediated by Ca(2+)-regulated exocytosis of lysosomes. Cell 106, 157–169.
Roy D, Liston DR, Idone VJ, Di A, Nelson DJ, Pujol C, Bliska JB, Chakrabarti S, Andrews NW (2004). A process for controlling intracellular bacterial infections induced by membrane injury. Science 304, 1515–1518.
Rutherford LC, Nelson SB, Turrigiano GG (1998). BDNF has opposite effects on the quantal amplitude of pyramidal neuron and interneuron excitatory synapses. Neuron 21, 521–530.
Sankaranarayanan S, Ryan TA (2000). Real-time measurements of vesicle-SNARE recycling in synapses of the central nervous system. Nat Cell Biol 2, 197–204.
Schiavo G, Osborne SL, Sgouros JG (1998). Synaptotagmins: more isoforms than functions. Biochem Biophys Res Commun 248, 1–8.
Schiavo G, Stenbeck G, Rothman JE, Sollner TH (1997). Binding of the synaptic vesicle v-SNARE, synaptotagmin, to the plasma membrane t-SNARE, SNAP-25, can explain docked vesicles at neurotoxin-treated synapses. Proc Natl Acad Sci USA 94, 997–1001.
Shi SH, Hayashi Y, Petralia RS, Zaman SH, Wenthold RJ, Svoboda K, Malinow R (1999). Rapid spine delivery and redistribution of AMPA receptors after synaptic NMDA receptor activation. Science 284, 1811–1816.
Stevens CF, Sullivan JM (2003). The synaptotagmin C2A domain is part of the calcium sensor controlling fast synaptic transmission. Neuron 39, 299–308.
Sudhof TC (2002). Synaptotagmins: why so many. J Biol Chem 277, 7629–7632.
Sugita S, Han W, Butz S, Liu X, Fernandez-Chacon R, Lao Y, Sudhof TC (2001). Synaptotagmin VII as a plasma membrane Ca(2+) sensor in exocytosis. Neuron 30, 459–473.
Sutton RB, Davletov BA, Berghuis AM, Sudhof TC, Sprang SR (1995). Structure of the first C2 domain of synaptotagmin I: a novel Ca2+/phospholipid-binding fold. Cell 80, 929–938.
Tai CY, Mysore SP, Chiu C, Schuman EM (2007). Activity-regulated N-cadherin endocytosis. Neuron 54, 771–785.
Takamori S *et al*. (2006). Molecular anatomy of a trafficking organelle. Cell 127, 831–846.
Ullrich B, Li C, Zhang JZ, McMahon H, Anderson RG, Geppert M, Sudhof TC (1994). Functional properties of multiple synaptotagmins in brain. Neuron 13, 1281–1291.
Wang P, Chicka MC, Bhalla A, Richards DA, Chapman ER (2005). Synaptotagmin VII is targeted to secretory organelles in PC12 cells, where it functions as a high-affinity calcium sensor. Mol Cell Biol 25, 8693–8702.
Wienisch M, Klingauf J (2006). Vesicular proteins exocytosed and subsequently retrieved by compensatory endocytosis are nonidentical. Nat Neurosci 9, 1019–1027.
Xu J, Mashimo T, Sudhof TC (2007). Synaptotagmin-1, -2, and -9: Ca(2+) sensors for fast release that specify distinct presynaptic properties in subsets of neurons. Neuron 54, 567–581.